# A Reynolds Number dependent Convergence Estimate for the Parareal Algorithm

Martin J. GANDER, Thibaut LUNET

## 1 The Parareal algorithm

Time parallel time integration has received substained attention over the last decades, for a review, see [2]. More recently, renewed interest in this area was sparked by the invention of the Parareal algorithm [5] for solving initial value problems like

$$\frac{d\boldsymbol{u}}{dt} = \mathcal{L}_h(\boldsymbol{u}(t),t), \;\; \boldsymbol{u}(0) = \boldsymbol{u}_0, \;\; t \in [0,T], \tag{1}$$

with $\mathcal{L}_h : \mathbb{R}^p \times \mathbb{R}^+ \to \mathbb{R}^p$, $\boldsymbol{u}(t) \in \mathbb{R}^p$, $\boldsymbol{u}_0 \in \mathbb{R}^p$, $p$ being the total number of degrees of freedom and $T$ a positive real value. Problem (1) often arises from the spatial discretization of a (non-)linear system of partial differential equations (PDEs) through the method-of-lines. For Parareal, one decomposes the global time interval $[0,T]$ into $N$ time subintervals $[T_{n-1},T_n]$ of size $\Delta T$, $n = 1,\cdots,N$, where $N$ is the number of processes to be considered for the time parallelization. In the following, we denote by $\boldsymbol{U}_n$ the approximation of $\boldsymbol{u}$ at time $T_n$, *i.e.* , $\boldsymbol{U}_n \approx \boldsymbol{u}(T_n)$. Let $\underset{T_{n-1}\to T_n}{\mathcal{F}^{\delta t}}(\boldsymbol{U}_{n-1})$ denote the result of approximately integrating (1) on the time subinterval $[T_{n-1},T_n]$ from a given starting value $\boldsymbol{U}_{n-1}$ using a fine propagator $\mathcal{F}$ with time step $\delta t$. Similarly, Parareal also needs a coarse propagator $\mathcal{G}$ with time step $\Delta t$), which has to be much cheaper than $\mathcal{F}$ resulting in less accuracy.

The Parareal algorithm consists of a prediction step and a correction iteration. In the prediction step, Parareal computes an inital guess of the starting values $\boldsymbol{U}_n^0$ at the beginning of each time subinterval using the coarse propagator,

$$\forall n = 1,\cdots,N, \;\; \boldsymbol{U}_n^0 = \underset{T_{n-1}\to T_n}{\mathcal{G}^{\Delta t}}(\boldsymbol{U}_{n-1}^0), \;\; \boldsymbol{U}_0^0 = \boldsymbol{u}_0. \tag{2}$$

Martin J. GANDER
University of Geneva, 2-4 rue du Lièvre, 1211 Genève 4, Suisse, e-mail: martin.gander@unige.ch

Thibaut LUNET
University of Geneva, 2-4 rue du Lièvre, 1211 Genève 4, Suisse, e-mail: thibaut.lunet@unige.ch

A correction iteration is then applied in PARAREAL, using concurrently the fine propagator $\mathcal{F}$ on each time subinterval:

$$\boldsymbol{U}_n^k = \underset{T_{n-1}\to T_n}{\mathcal{F}^{\delta t}}(\boldsymbol{U}_{n-1}^{k-1}) + \underset{T_{n-1}\to T_n}{\mathcal{G}^{\Delta t}}(\boldsymbol{U}_{n-1}^{k}) - \underset{T_{n-1}\to T_n}{\mathcal{G}^{\Delta t}}(\boldsymbol{U}_{n-1}^{k-1}), \tag{3}$$

where $\boldsymbol{U}_n^k$ denotes the approximation of $\boldsymbol{u}$ at time $T_n$ at the $k$-th iteration of PARAREAL ($k = 1, \cdots, K$, $n = 1, \cdots, N$). While the application of $\mathcal{F}$ can be performed independently for each time subinterval, PARAREAL remains limited by the sequential nature of the coarse integration performend by $\underset{T_{n-1}\to T_n}{\mathcal{G}^{\Delta t}}$ in (3). PARAREAL will thus reduce the total computational time compared to a direct time-serial integration only if the application of $\mathcal{G}$ is cheap enough and if the total number of iterations $K$ of PARAREAL is small. We will use the following result, which is an extension of [4, Th. 4.9] following indications of [4, Sec. 4.5] for the Dahlquist test equation

$$\frac{du}{dt} = \lambda u, \quad \lambda \in \mathbb{C}, \quad u(0) = u_0 \in \mathbb{C}. \tag{4}$$

**Theorem 1 (Linear convergence bound - Dahlquist test equation)** *Let $\mathcal{G}$ be a one-step time-integration method, and $\mathcal{F}$ be the same time integrator, but using $m$ time-steps instead of a single one (i.e. $\Delta t = \Delta T = m\delta t$). If $\mathcal{G}$ is used such that $\lambda\Delta t$ is in its region of absolute stability, then*

$$\sup_{n>0} |u_n^{\mathcal{F}} - U_n^k| \leq \rho(\lambda\Delta T)^k \sup_{n>0} |u_n^{\mathcal{F}} - U_n^0|, \tag{5}$$

*where $u_n^{\mathcal{F}}$ is the fine solution a time $T_n$, and the* convergence factor *is given by*

$$\rho(\lambda\Delta T) = \frac{|R(\lambda\Delta T/m)^m - R(\lambda\Delta T)|}{1 - |R(\lambda\Delta T)|}, \tag{6}$$

*with $R$ the stability function of the coarse (and fine) solver.*

## 2 Semi-discretization of the advection-diffusion problem

We are interested in the linear advection-diffusion equation on a one-dimensional spatial domain $[0, L]$

$$\frac{\partial u}{\partial t} = -a\frac{\partial u}{\partial x} + \nu\frac{\partial^2 u}{\partial x^2} + f(x,t), \quad u(x,0) = u_0(x), \tag{7}$$

with $a, \nu \in \mathbb{R}_+^*$ the advection and diffusion coefficients, $f : \mathbb{R} \times \mathbb{R}^+ \to \mathbb{R}$ a source term, and periodic boundary conditions for the spatial domain

$$\forall t \in [0,T], \quad u(0,t) = u(L,t). \tag{8}$$

We discretize $[0, L]$ using a uniform mesh $[x_1, ..., x_p]^T$ for $p$ unknowns, which gives a mesh size $\delta_x = L/p$. We use centered finite differences of order 2 (FD-C2) for the diffusion operator in (7), and also use either a FD-C2 discretization for the advection operator, or a $1^{st}$ order upwind scheme (FD-U1). This leads to the semi-discrete system of ODEs

$$\frac{d\boldsymbol{u}}{dt}(t) = A\boldsymbol{u}(t) + \boldsymbol{f}(t), \;\; \boldsymbol{u}(0) = \boldsymbol{u}_0, \tag{9}$$

where $A \in \mathbb{R}^{p\times p}$ and $\boldsymbol{f} : \mathbb{R} \to \mathbb{R}^p$ represents the source term.

Two dimensionless numbers can be defined to characterize this problem:

$$Re := \frac{aL}{\nu}, \;\; Re_{\delta_x} := \frac{a\delta_x}{\nu}, \tag{10}$$

where $Re$ is the Reynolds number[1] and $Re_{\delta_x}$ is the mesh Reynolds number ($Re = pRe_{\delta_x}$). $Re$ indicates by its large (resp. small) value a major influence of advection (resp. diffusion) on the solution $u(x,t)$. As $Re$ compares this advection/diffusion ratio with the characteristic length $L$ (that can be chosen differently for a different situation), $Re_{\delta_x}$ compares this ratio to the mesh size. Decreasing the diffusion coefficient will increase $Re$, as the advection becomes more dominant. It does not necessarily induce an increase of $Re_{\delta_x}$, as $\delta_x$ can also be decreased to keep a constant value for $Re_{\delta_x}$. This mesh refinement when $Re$ increases is commonly done for Direct Numerical Simulation (DNS) of the Navier-Stokes equations [6, Chap. 4], or also for stationary forms of (9) with Dirichlet boundary conditions, to keep a certain accuracy in the approximate solution (solutions become qualitatively wrong when $Re_{\delta_x} \geq 2$ for FD-C2 dicretizations of the advection term [1, Sec. 2, § 5]).

The mesh Reynolds number $Re_{\delta_x}$ is useful to formulate convergence results for Parareal. In particular, we can use it to express the eigenvalues of $A$ in (9):

**Lemma 1 (Eigenvalues of the spatial advection-diffusion operator)**
*For the FD-C2 discretization of the diffusion term with periodic boundary conditions, the eigenvalues of the discrete spatial operator A with FD-C2 discretization of the advection are*

$$\lambda_\kappa = -\frac{a}{\delta_x}\left[i\sin\left(\frac{2\kappa\pi}{p}\right) + \frac{2}{Re_{\delta_x}}\left(1-\cos\left(\frac{2\kappa\pi}{p}\right)\right)\right], \;\; \kappa \in \{0, 1, ..., .., p-1\}, \tag{11}$$

*with* $i := \sqrt{-1}$. *For the FD-U1 discretization of the advection, the eigenvalues are*

$$\lambda_\kappa = -\frac{a}{\delta_x}\left[1 - e^{-i\frac{2\kappa\pi}{p}} + \frac{2}{Re_{\delta_x}}\left(1-\cos\left(\frac{2\kappa\pi}{p}\right)\right)\right], \;\; \kappa \in \{0, 1, ..., .., p-1\}. \tag{12}$$

*Proof* For the FD-C2 discretization of the advection term, the space operator matrix is given by

[1] What we call here the Reynolds number is in fact the Peclet number, since there is no non-linear advective term in (7). However, we prefer to use Reynolds number, since our analysis is a first step toward Navier-Stokes equations, and this links our results to those already in the literature.

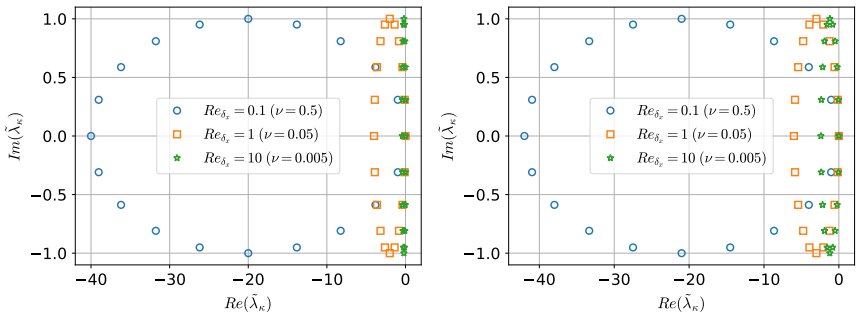


*Fig. 1: Influence of $Re_{\delta_x}$ on the eigenvalues of the advection-diffusion problem when varying $\nu$ only and keeping $a$ and $\delta_x$ fixed. For the advection term, we used FD-C2 (left) and FD-U1 (right), with $p = 20$, $a = 1$, $L = 1$, and for the axes, we used $\tilde{\lambda}_\kappa := \delta_x / a\lambda_\kappa$.*

$$A := -\frac{a}{2\delta_x}\begin{pmatrix} 0 & 1 & & -1 \\ -1 & \ddots & \ddots & \\ & \ddots & \ddots & 1 \\ 1 & & -1 & 0 \end{pmatrix} + \frac{\nu}{\delta_x^2}\begin{pmatrix} -2 & 1 & & 1 \\ 1 & \ddots & \ddots & \\ & \ddots & \ddots & 1 \\ 1 & & 1 & -2 \end{pmatrix}, \tag{13}$$

where the eigenvalues of each matrix are well known (see, *e.g.* [6, Chap. 3]). Each circulant matrix is diagonalized by the same Fourier basis, and hence the eigenvalues $\lambda_\kappa$ of $A$ are just the sum of the eigenvalues of each matrix in (13), i.e.

$$\lambda_\kappa = -i\frac{a}{2\delta_x}\sin(2\kappa\pi/p) + 2\frac{\nu}{\delta_x^2}\left(1 - \cos\left(\frac{2\kappa\pi}{p}\right)\right). \tag{14}$$

Extracting the common factor $a/\delta_x$ and using the definition of $Re_{\delta_x}$ then leads to (11). The result for FD-U1 in (12) is obtained similarly. □

In Fig. 1, we show the eigenvalues for both discretizations, FD-C2 and FD-U1, and their dependency on $Re_{\delta_x}$ when varying $\nu$ only. We see that the eigenvalues are distributed along an ellipse that flattens toward the imaginary axis when $Re_{\delta_x}$ increases. For small $Re_{\delta_x}$, the eigenvalues are very similar, but for large $Re_{\delta_x}$, the flattening toward the imaginary axis is more pronounced for FD-C2 than for FD-U1, which comes from the numerically more diffusive nature of FD-U1.

## 3 Linear bound of PARAREAL for advection-diffusion

**Theorem 2 (Linear convergence bound - Advection-diffusion equation)** *Let $\mathcal{G}$ be a one-step time-integration method, $\mathcal{F}$ be the same time integrator using $m$ time-steps, and $\boldsymbol{u}_n^{\mathcal{F}}$ be the fine sequential solution at $T_n$. If $\lambda_\kappa \Delta T$ is in the region of absolute stability of $\mathcal{G}$ for each eigenvalue $\lambda_\kappa$ of $A$, then the error in the PARAREAL algorithm*

*satisfies the linear error bound*

$$E_\infty^k := \sup_{n>0} \left\| \boldsymbol{u}_n^{\mathcal{F}} - \boldsymbol{U}_n^k \right\|_2 \leq \rho_{ad}^k C_\infty^0, \;\; C_\infty^0 = \sqrt{\sum_\kappa \sup_{n>0} \left| \hat{u}_n^{\mathcal{F}}(\kappa) - \hat{U}_n^0(\kappa) \right|^2} \tag{15}$$

*where $\hat{u}(\kappa)$ is the $\kappa^{th}$ Fourier component of $\boldsymbol{u}$ and $\rho_{ad}$ denotes the* linear convergence factor *of Parareal,*

$$\rho_{ad} = \sup_{\lambda_\kappa}[\rho(\lambda_\kappa \Delta T)] = \sup_{\lambda_\kappa} \left[ \frac{|R(\lambda_\kappa \Delta T/m)^m - R(\lambda_\kappa \Delta T)|}{1 - |R(\lambda_\kappa \Delta T)|} \right], \tag{16}$$

*with R the stability function of the coarse (and fine) solver. In particular, Parareal convergence is ensured if $\rho_{ad} < 1$.*

*Proof* As the unitary Discrete Fourier Transform (DFT) matrix transforms $A$ into diagonal form, (9) is then a combination of decoupled Dahlquist equations in Fourier space. Using Theorem 1, we can bound the Parareal error of each Fourier component for all time subintervals,

$$\forall n \in \mathbb{N}, \;\; |\hat{u}_n^{\mathcal{F}}(\kappa) - \hat{U}_n^k(\kappa)| \leq \sup_{n>0} |\hat{u}_n^{\mathcal{F}}(\kappa) - \hat{U}_n^k(\kappa)| \leq \rho(\lambda_\kappa \Delta T)^k \sup_{n>0} |\hat{u}_n^{\mathcal{F}}(\kappa) - \hat{U}_n^0(\kappa)|. \tag{17}$$

For each $\kappa$, $\rho(\lambda_\kappa \Delta T)$ can be bounded by $\sup_{\lambda_\kappa}[\rho(\lambda_\kappa \Delta T)]$. Then, taking the power 2 of each extremal part of the inequality, summing on $\kappa$ and computing the square root gives

$$\left\| \hat{\boldsymbol{u}}_n^{\mathcal{F}} - \hat{\boldsymbol{U}}_n^k \right\|_2 \leq \sup_{\lambda_\kappa}[\rho(\lambda_\kappa \Delta T)]^k C_\infty^0 \tag{18}$$

Using the Parseval-Plancherel theorem and bounding the left term for $n \in \mathbb{N}$ then leads to (15). □

As we saw previously, the eigenvalues $\lambda_\kappa$ are fully characterized by $Re_{\delta_x}$ and $a/\delta_x$. Hence, we can define a dimensionless number,

$$CFL_{\mathcal{P}} = \frac{a \Delta T}{\delta_x}, \tag{19}$$

which we call Courant-Friedrichs-Lewy (CFL) number for Parareal (as if the algorithm were simply considered as a standard time integration method with time-step $\Delta T$). It is worth mentioning that $CFL_{\mathcal{P}}$ is the CFL number of the coarse solver, and $m$ times the CFL number of the fine solver, and we obtain the following result:

**Lemma 2** *For a given mesh with p mesh points, the linear convergence factor $\rho_{ad}$ of Parareal for the advection-diffusion equation in* (16) *depends only on $Re_{\delta_x}$, $CFL_{\mathcal{P}}$, and the coarse/fine solver settings, i.e. the stability function R and the number of time-steps m per time subinterval.*

*Proof* Looking for example at the FD-C2 discretization for advection, combining (19) with (11), we get

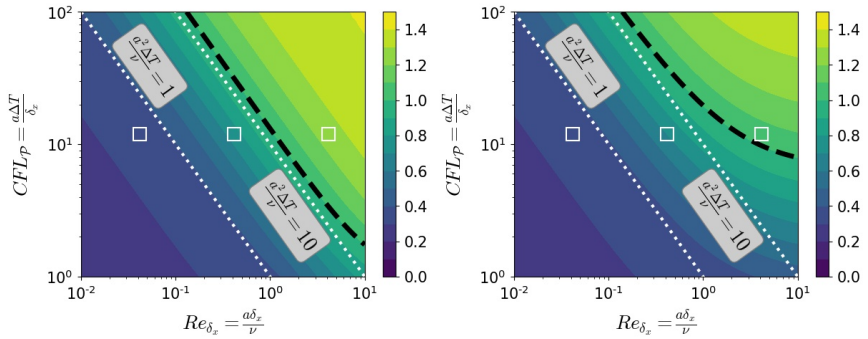


*Fig. 2: Dependence of $\rho_{ad}$ on $Re_{\delta_x}$ and $CFL_{\mathcal{P}}$, for Backward Euler ($m = 30$ for $\mathcal{F}$), and FD-C2 (left) and FD-U1 (right). Dotted black line: $\rho_{ad} = 1$. White squares are $(Re_{\delta_x}, CFL_{\mathcal{P}})$ tuples used in Sec. 4. White dotted lines are $(Re_{\delta_x}, CFL_{\mathcal{P}})$ values for some given constant ratio $a^2\Delta T/\nu$.*

$$\lambda_\kappa \Delta T = -CFL_{\mathcal{P}} \left[ i \sin\left(\frac{2\kappa\pi}{p}\right) + \frac{2}{Re_{\delta_x}}\left(1 - \cos\left(\frac{2\kappa\pi}{p}\right)\right)\right], \quad \kappa \in \{0, 1, ..., .., p-1\}, \tag{20}$$

which depends only on $\kappa$, $Re_{\delta_x}$ and $CFL_{\mathcal{P}}$. As $\rho_{ad}$ is a maximum bound over all $\kappa$, we obtain the result from (16). The proof is similar for FD-U1. □

We present the dependency proved in Lemma 2 graphically using contour plots for $\rho_{ad}$ in Fig. 2, with a Backward Euler time integrator for $\mathcal{F}$ and $\mathcal{G}$, using $m = 30$ and $p = 5000$. For both discretizations, we observe an increase of $\rho_{ad}$ with both $Re_{\delta_x}$ and $CFL_{\mathcal{P}}$, in agreement with numerical results in the literature (see, *e.g.* , [3]). Our analysis quantifies this convergence deterioration, and shows how $\rho_{ad}$ depends precisely on $Re_{\delta_x}$ and $CFL_{\mathcal{P}}$. Furthermore, for sufficient space resolution (small $Re_{\delta_x}$), $\rho_{ad}$ is determined by $CFL_{\mathcal{P}} Re_{\delta_x} = a^2\Delta T/\nu$ (white dotted lines in Fig. 2). In particular, convergence is only ensured when $a^2\Delta T/\nu$ is less than a given value (around 10 in our case). This implies that $\Delta T$ must be in the order of $\nu/a^2$, or in other words, the coarse time step must be small enough for $\mathcal{G}$ to capture the diffusion time-scale, requiring that $\mathcal{G}$ has an $\mathcal{F}$-like resolution.

Using the FD-U1 discretization only changes the convergence factor for large values of $Re_{\delta_x}$, which may not be of use since $Re_{\delta_x} >> 1$ can lead to an important loss of accuracy for the numerical solution, as we will see in Sec. 4.

## 4 Numerical experiments

We perform now numerical experiments similar to those already in the literature (see, *e.g.* , [7, 3]), where we use a fixed number of mesh points $p$, and decrease the diffusion coefficient $\nu$ to obtain larger values of $Re$, for a fixed value $a = 1$ of the advection. Numerical simulations are done with $L = 2$ and $p = 48$, until $T = 4$. Backward Euler is used for the $\mathcal{F}$ and $\mathcal{G}$ solvers, with $m = 30$. Since we

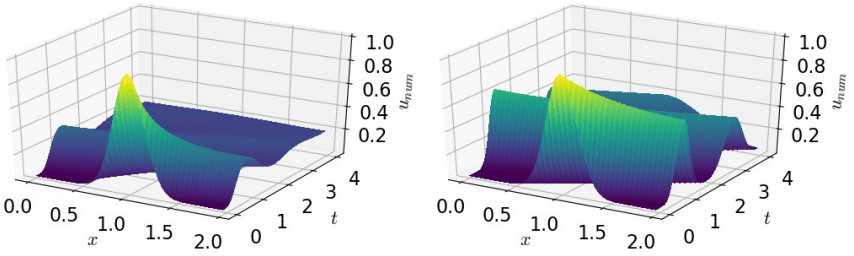


*Fig. 3: Space-time numerical solution with the $\mathcal{F}$ solver using FD-C2 for the advection discretization. Left: $\nu = 0.1$ ($Re = 20$), right: $\nu = 0.01$ ($Re = 200$).*

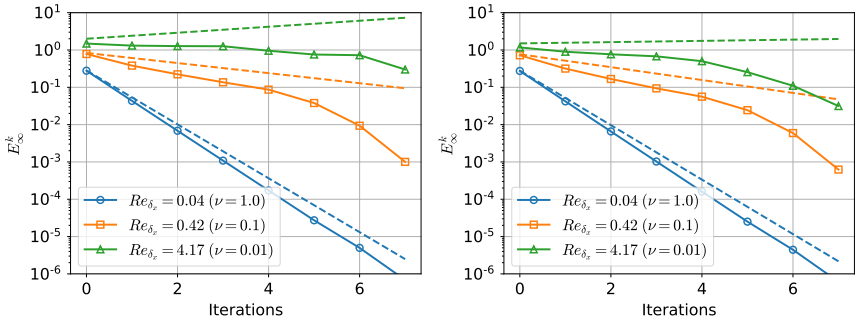


*Fig. 4: Influence of an increase of $Re_{\delta_x}$ by lowering $\nu$ on PARAREAL convergence, using FD-C2 for the advection discretization (left) and FD-U1 (right), linear bounds in dotted lines.*

use $N = 8$ time subintervals for PARAREAL, this implies a fine time step $\delta_t = 1/60$ and $CFL_{\mathcal{P}} = 12$. We use a Gaussian as initial condition, $u_0(x) = e^{-20(x-1)^2}$, and no source term. Three different viscosity coefficients are chosen, $\nu \in \{1, 0.1, 0.01\}$. Numerical solutions are shown in Fig. 3 for the two smaller values of $\nu$; for the largest value $\nu = 1$, the solution is almost purely diffusive, and is constant for $t > 1$. We show in Fig. 4 the error against the fine solution at each PARAREAL iteration, using the FD-C2 and FD-U1 discretizations. For each $Re_{\delta_x}$ value corresponding to the chosen $Re$, the linear bound is indicated by the dashed lines, and the corresponding $(CFL_{\mathcal{P}}, Re_{\delta_x})$ tuples are indicated with the white squares in Fig. 2. We observe for both discretizations a degradation of the PARAREAL convergence when $\nu$ decreases and thus $Re$ and $Re_{\delta_x}$ increase, which is well predicted by the linear convergence bound (dashed lines in Fig. 4). The use of the FD-U1 discretization lessens this convergence degradation a little for high $Re_{\delta_x}$ numbers (low $\nu$), which is due to the artificial dissipation brought by the Upwind scheme that makes the problem (wrongly) more diffusive.

This loss of accuracy is particularly visible when comparing the fine solution to the analytical solution of (7) with periodic boundary conditions, $u(x,t) = \frac{1}{\sqrt{4\pi\nu t}} \int_{-\infty}^{+\infty} u_0(\xi) \exp(-\frac{(x-at-\xi)^2}{4\nu t}) d\xi$. We define the numerical error "in time and

*Table 1: Main parameters for the numerical experiments*

| $\nu$ | $Re$ | $Re_{\delta_x}$ | $\epsilon_{T,S}$ (FD-C2) | $\epsilon_{T,S}$ (FD-U1) |
|---|---|---|---|---|
| 1 | 2 | 0.042 | 0.006 | 0.005 |
| 0.1 | 20 | 0.42 | 0.040 | 0.096 |
| 0.01 | 200 | 4.2 | 0.321 | 0.724 |

space" of the fine solution $\epsilon_{T,S} := \frac{1}{N_{step}} \sum_{i=1}^{N_{step}} ||\boldsymbol{u}^{ref}(i\delta_t) - \boldsymbol{u}^{\mathcal{F}}(i\delta_t)||_2$, where $N_{step}$ is the number of time steps for the fine solver to cover $[0,T]$ (in our case, $N_{step} = 240$), and $\boldsymbol{u}^{ref}$ is the analytical solution computed at each mesh point. We give $\epsilon_{T,S}$ for each discretization and $Re_{\delta_x}$ in Tab. 1. One can see that the accuracy decreases dramatically when $Re$ and $Re_{\delta_x}$ increase, the effect being more important for the FD-U1 discretization, compared to the FD-C2 discretization. In order to reduce this error, a mesh refinement would be necessary, which would have led to lower $Re_{\delta_x}$ values for the chosen $Re$, but also to corresponding higher values of $CFL_{\mathcal{P}}$, thus not changing anything in the convergence behavior of the method (*cf.* white dotted lines in Fig. 2).

In conclusion, both our theoretical results and our numerical experiments show that parareal algorithm convergence deteriorates when the Reynolds number becomes large. One also has to be careful when using numerically diffusive schemes not to jump to false conclusions: truly transport dominated solutions are hard to approximate effectively with the classical parareal algorithm.

## References

1. Birkhoff, G., Gartland Jr, E., Lynch, R.: Difference methods for solving convection-diffusion equations. Computers & Mathematics with Applications **19**(11), 147–160 (1990)
2. Gander, M.J.: 50 years of time parallel time integration. In: T. Carraro, M. Geiger, S. Körkel, R. Rannacher (eds.) Multiple Shooting and Time Domain Decomposition Methods, pp. 69–114. Springer (2015)
3. Gander, M.J.: Five decades of time parallel time integration, and a note on the degradation of the performance of the Parareal algorithm as a function of the Reynolds number. Oberwolfach Report (2017)
4. Gander, M.J., Vandewalle, S.: Analysis of the Parareal time-parallel time-integration method. SIAM J. Sci. Comput. **29**(2), 556–578 (2007)
5. Lions, J.L., Maday, Y., Turinici, G.: A "Parareal" in time discretization of PDE's. C. R. Math. Acad. Sci. Paris **332**(7), 661–668 (2001)
6. Lunet, T.: Stratégies de parallélisation espace-temps pour la simulation numérique des écoulements turbulents. Ph.D. thesis, Toulouse, ISAE (2018)
7. Steiner, J., Ruprecht, D., Speck, R., Krause, R.: Convergence of Parareal for the Navier-Stokes equations depending on the Reynolds number. In: A. Abdulle, S. Deparis, D. Kressner, F. Nobile, M. Picasso (eds.) Numerical Mathematics and Advanced Applications - ENUMATH 2013, vol. 103, pp. 195–202. Springer (2015)